

FIRST RESULTS FROM THE HIGH RESOLUTION  
POWDER DIFFRACTOMETER HRPD AT THE SNS

W I F David and M W Johnson

Neutron Division  
Rutherford Appleton Laboratory  
Chilton, Didcot, Oxon, OX11 0QX, UK

INTRODUCTION

The High Resolution Powder Diffractometer (HRPD) at the SNS is the first of a new generation of high-flux neutron powder diffractometers to exploit resolutions of under  $10^{-3}$ . The first results, after two weeks of commissioning, have been very promising and have confirmed the major aspects of the instrument. Data have been collected at high ( $\Delta d/d \approx 4 \times 10^{-4}$ ) and (comparatively) low ( $\Delta d/d \approx 10^{-3}$ ) resolution positions from samples of Ni, NiO and Si powders. Several new observations have been obtained, as a consequence of the uniquely high resolution of HRPD, from preliminary analysis of the six data sets.

In order to achieve ( $\Delta d/d$ ) resolutions of the order of  $4 \times 10^{-4}$  the primary flight path of the diffractometer must be of the order of 100 m. At the SNS design pulse repetition frequency of 50 Hz this introduces problems of frame overlap that have been circumvented by using two beam choppers. However, in the initial commissioning period the lower repetition rates of between 50/16 Hz and 50/64 Hz have produced no severe frame overlap problems.

The primary flight path of HRPD has been enclosed within a curved nickel glass guide tube of cross-section 8 cm x 2.5 cm to attenuate the  $\gamma$ -rays and fast neutrons associated with the initial neutron burst. The curved section of the guide tube, which extends from 6 m to 60 m from the moderator, has a radius of curvature of 18 km. These parameters represent

the optimised configuration for a 50 Hz source in which no line of sight neutrons reach the sample yet the radius of curvature is sufficiently shallow to allow transmission of sub-angstrom neutrons. The 60 m - 96 m straight section of the guide is necessary to smooth out beam intensity inhomogeneities in the guide. Figure 1 shows the observed and calculated fluxes (curve A) at the sample extrapolated to full SNS intensity. No neutrons are transmitted with  $\lambda \lesssim 0.5 \text{ \AA}$  whilst for  $\lambda > 5 \text{ \AA}$  the flux varies as  $\sim \lambda^{-5}$ . Curve B gives the expected flux at 100 m in the absence of a guide. It is evident from comparison of curves A and B that the use of a guide has produced a substantial increase in flux at the sample by allowing neutrons to be carried over the long flight path without the usual inverse square loss of intensity. Indeed at  $1 \text{ \AA}$  and  $2 \text{ \AA}$  the flux expected for HRPD are roughly equivalent to 30 m and 15 m machines respectively.

A schematic drawing of HRPD is given in Figure 2. Two sample positions are available, at 1 m and 2 m from the backscattering bank of detectors, with vertical access to both positions for sample environment instrumentation. The backscattering detector at present consists of two of a final eight octants that form a series of 20 concentric detector rings. This fibre-optic encoded position sensitive detector, constructed at the Rutherford Appleton Laboratory, detects neutrons by scintillation within a Li-doped cerium glass. The concentric geometry of detector matches that of the Debye-Scherrer cones thereby eliminating geometrical contributions to the profile line shape. Further details are summarised in Table 1.

The resolution of HRPD results from a combination of different physical variables and a detailed discussion of the matching of different instrument parameters will be given elsewhere (1). A simplified account of the resolution contributions to  $(\Delta d/d)$  begins with the assumption that all variables are independent and that

$$\frac{\Delta d}{d}^2 = \frac{\Delta t}{t}^2 + \frac{\Delta \ell}{\ell}^2 + (\Delta \theta \cot \theta)^2 + \frac{d}{p}^2$$

$(\Delta t/t)$  arises from the time distribution of the neutron pulse resulting from the moderator. Moderator optimisation studies (eg. (2)) has led to the decision to use a 10 x 10 cm 95 K poisoned methane moderator.  $\Delta t$  ( $\mu\text{sec}$ ) is of the order of  $8\lambda(\text{\AA})$  giving a resolution contribution  $(\Delta t/t) \sim 0.03\%$  for a 98 m instrument.  $\Delta \ell$  is the uncertainty in the flight path  $\ell$  and results from finite sample (1.0 cm) and detector (0.5 cm)

widths. For  $\ell = 98$  m this is of the order of  $(\Delta\ell/\ell) = 0.01\%$ . The angular uncertainty  $\Delta\theta \cot\theta$  resulting from sample and detector size is only small for  $\theta > 85^\circ$  thus necessitating a high angle backscattering bank. At the 1 m position the angular resolution of the 10th detector ring is 0.06% while for the 2 m position  $(\Delta\theta \cot\theta) \sim 0.015\%$ . Thus neglecting particle size effects ( $d/p$  where  $d = d$  spacing of reflection and  $p =$  particle diameter)

$$(\Delta d/d)^2 \sim 0.1\% \quad 1 \text{ m position}$$

$$(\Delta d/d)^2 \sim 0.04\% \quad 2 \text{ m position}$$

There is thus a significant geometrical contribution to the 1 m but not the 2 m position. This gives the experimenter a choice between a higher resolution (2 m position) or higher intensity configuration (1 m position). The backscattered flux intercepted by the detector with the 1 m sample position is roughly 4 times that at 2 m.

#### INITIAL COMMISSIONING EXPERIMENTS

In the initial commissioning period (2nd - 28th July 1985) calibration experiments have been performed using 3 samples (Ni, NiO and Si) at both high and low resolution positions on HRPD. A selection of the results obtained so far are presented in the following sections:

##### Nickel

Figure 3 shows the Ni 111 reflection individually plotted for each of the 20 concentric rings of one detector octant. The differing times of arrival of the 111 reflection arise because of the differing  $2\theta$  values ( $160^\circ \leq 2\theta \leq 176^\circ$ ) for the detector rings. Figure 3b highlights the expected exponentially-decaying trailing edge: Figure 3a, however, shows a pronounced leading edge unanticipated from instrumental considerations. Subsequent analysis at the higher resolution 2 m position (Figures 4a and b) revealed that the leading edge has a Lorentzian character. The convolution of exponential and Lorentzian functions gave a significantly improved fit over the conventional exponential/Gaussian convolution. The Lorentzian character may be attributed to particle-size effects: a straightforward calculation yields a domain size of  $1710(70) \text{ \AA}$ .

## Nickel Oxide

Antiferromagnetic NiO was chosen since, at room temperature, cubic rocksalt symmetry is lost and the structure appears to be rhombohedral. High resolution x-ray diffraction has established that the rhombohedral unit cell constants are  $a = 4.1758 \text{ \AA}$ ,  $\alpha = 90.058(2)^\circ$ . To observe the resultant splitting of Bragg peaks requires a resolution of less than 0.001. The profiles presented in Figures 5 and 6 clearly indicate that this resolution has been achieved. The splittings of 75  $\mu\text{s}$  and 82  $\mu\text{s}$  in Figures 6a and b correspond respectively to unit cell angles of  $90.0591^\circ$  and  $90.0588^\circ$  that are in excellent agreement with the literature value.

## Silicon

The silicon standard material (NBS Si640a :  $a = 5.430825(11) \text{ \AA}$ ), Hubbard (1983)) has been used as a calibrant of the overall flight path of HRPD at the 1 m and 2 m positions. Surprisingly in common with the Ni diffraction patterns discussed above, the convolution of exponential and Lorentzian functions gives a fit that is significantly superior than the exponential/Gaussian convolution (Figure 7) for all diffraction peaks. The linear variation with time (d-spacing) (Figure 8) of the full width at half maximum of the Lorentzian component of the fitted peak shape precludes particle-size effects suggesting rather that the Si standard sample suffers from Lorentzian strain broadening of the order of  $10^{-4}$ . These results highlight the fact that the high instrumental resolution of HRPD will not only prove advantageous for structure refinement but, additionally, will yield further information about the strain and size distributions of crystallites.

## INITIAL CONCLUSIONS

The initial commissioning experiments have proved extremely fruitful and have allowed the following aspects of the machine to be validated:

- Verification of poisoned moderator characteristics: 35  $\mu\text{s}$  decay constant observed in peak shape.
- Satisfactory alignment of neutron guide: wavelength cutoff = 0.48  $\text{\AA}$ .
- No observable cross-talk and acceptable quiet counts ( $\sim 1 \text{ count cm}^{-2} \text{ min}^{-1}$ ) in encoded scintillator detectors.

- Observation of NiO rhombohedral splitting ( $\Delta d/d$  full-width at half maximum of  $4 \times 10^{-4}$  measured).
- No observed splitting of NiO 200 reflection implying that NiO monoclinic splitting corresponds to a strain of less than  $2 \times 10^{-4}$ .
- Line broadening in Ni and Si diffraction patterns. (Exponential/Lorentzian convolution gives excellent least-squares fit of peak shapes).

#### ACKNOWLEDGEMENTS

The authors wish to acknowledge the help of numerous members of staff at the Rutherford Appleton Laboratory. Additionally, the authors wish to thank Dr A K Cheetham (University of Oxford) for suggesting NiO as a test material and providing the sample and M M Eddy (University of Oxford) for assistance with a number of the initial experiments.

#### REFERENCES

Hubbard, C. R., (1983) J. Appl. Cryst. 16 285-288.

TABLE 1 HRPD parameters

MODERATOR	10 x 10 cm CH <sub>4</sub> @ 95K.													
PRIMARY FLIGHT-PATH	96 m evacuated curved neutron guide.													
GUIDE PARAMETERS	width 2.5 cm height 8.0 cm length of sections = 1 m 4 m - 6.5 m straight 6.5 m - 60 m curved: r = 18 km 60 m - 100 m straight $\lambda^* = 0.98 \text{ \AA}$													
DISC CHOPPERS	At 6 m and 9 m. 3 apertures corresponding to 1, 2 or 5 frame apertures.													
DETECTOR TANK	Evacuated ( $10^{-1}$ torr normal, $10^{-6}$ available) light shielding. 2 sample positions at 1 m and 2 m from back-scattering detector.													
DETECTOR (eight octants)	<p>1. Back-scattering: 160 elements, 20 rings. <math>r_{\min} = 3 \text{ cm}</math> <math>r_{\max} = 37 \text{ cm}</math></p>	<table border="1"> <thead> <tr> <th></th> <th>1 m</th> <th>2 m</th> </tr> </thead> <tbody> <tr> <td><math>\Omega</math></td> <td>0.37</td> <td>0.1</td> </tr> <tr> <td><math>2\theta_{\min}</math></td> <td>160°</td> <td>170°</td> </tr> <tr> <td><math>2\theta_{\max}</math></td> <td>176°</td> <td>178°</td> </tr> </tbody> </table>		1 m	2 m	$\Omega$	0.37	0.1	$2\theta_{\min}$	160°	170°	$2\theta_{\max}$	176°	178°
	1 m	2 m												
$\Omega$	0.37	0.1												
$2\theta_{\min}$	160°	170°												
$2\theta_{\max}$	176°	178°												
MONITORS	2 monitors at - 250 cm and 105 cm from 2 m position.													
TIME SORTING	$n_t \leq 64K$ channel time boundaries software set.													

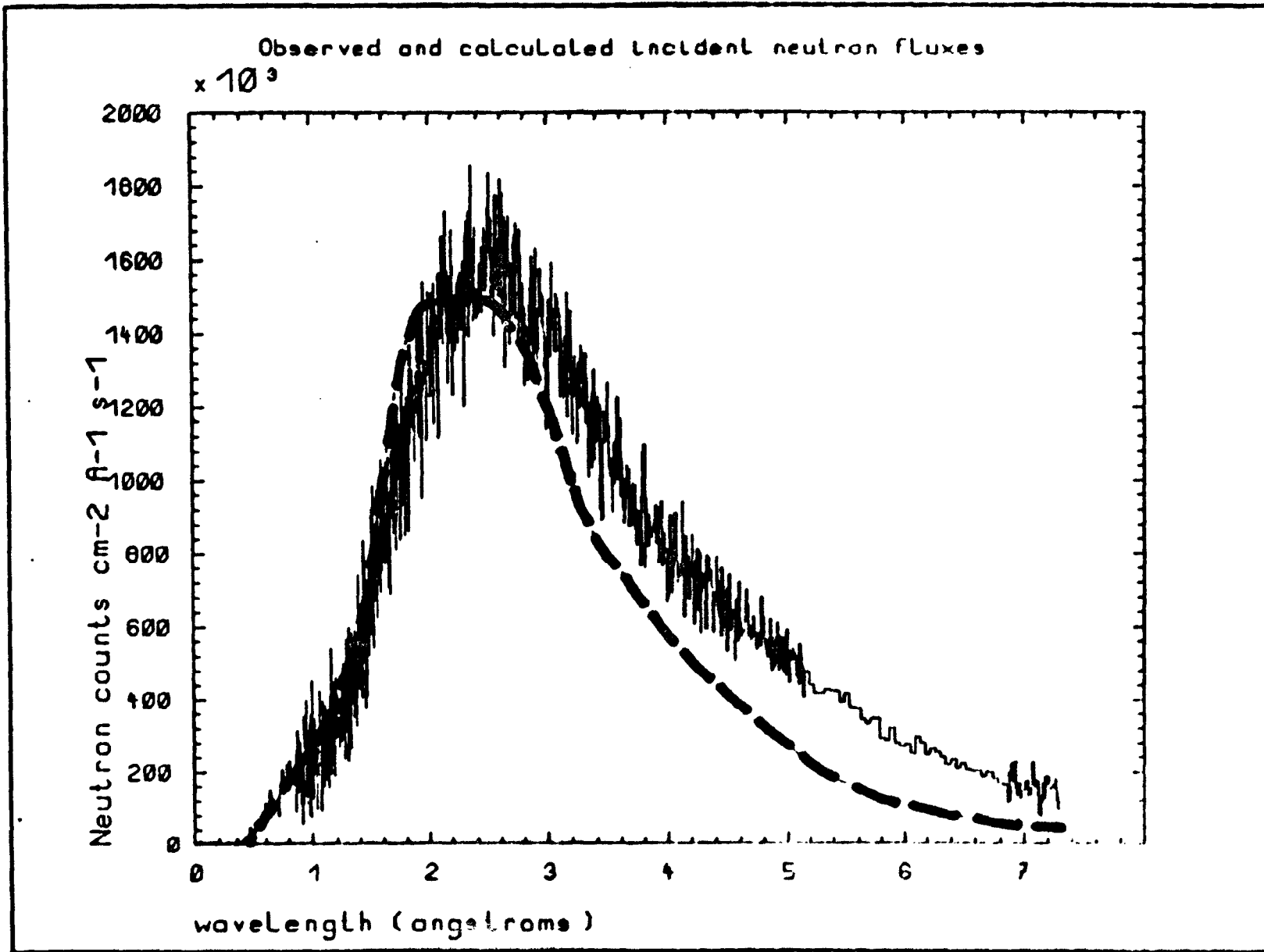
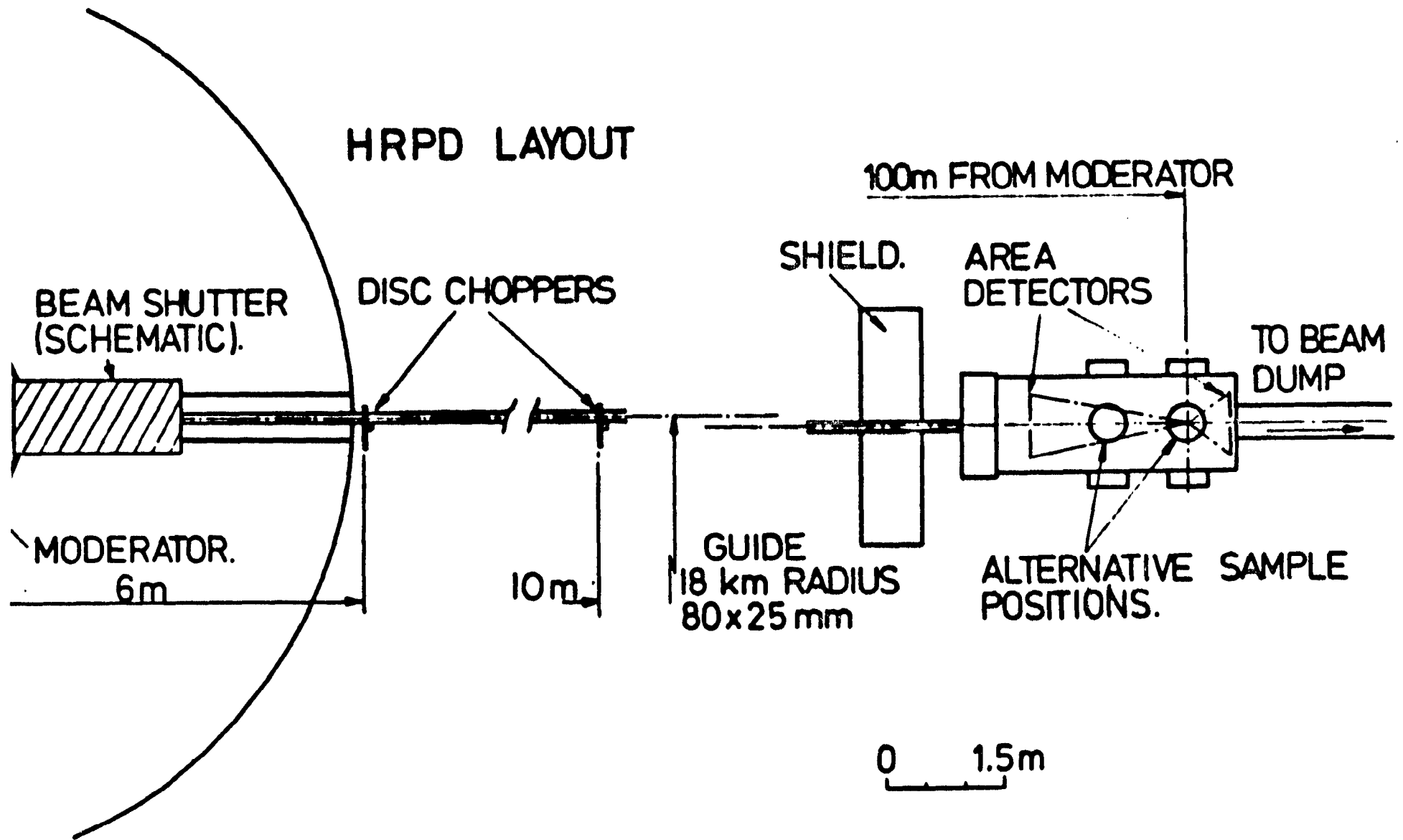


Figure 1: Observed and calculated neutron fluxes (extrapolated to full SNS intensity) for HRPD. Note the absence of epithermal neutrons below  $\lambda = 0.5 \text{Å}$ .



- 434 -

Figure 2: HRPD instrument configuration.



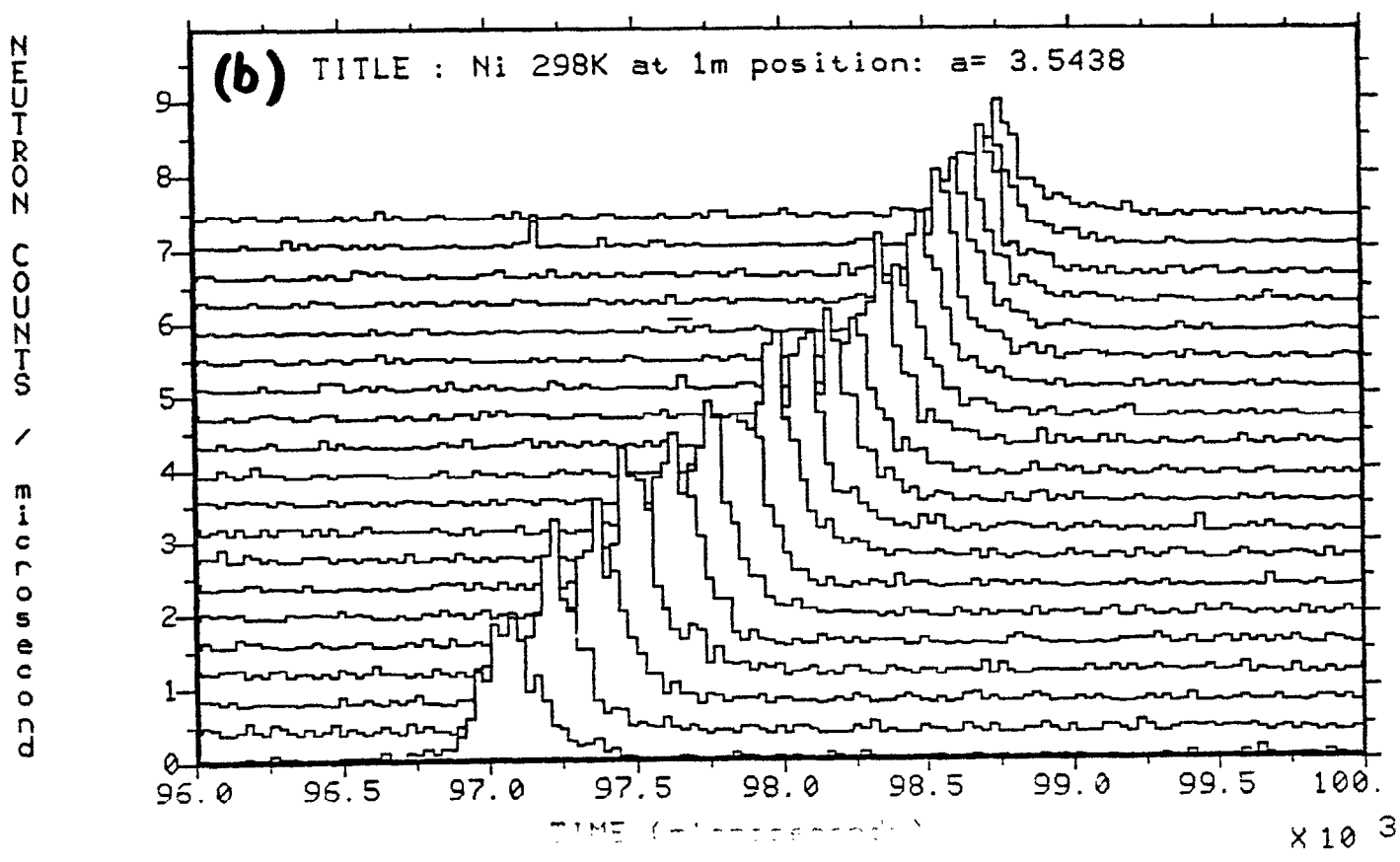
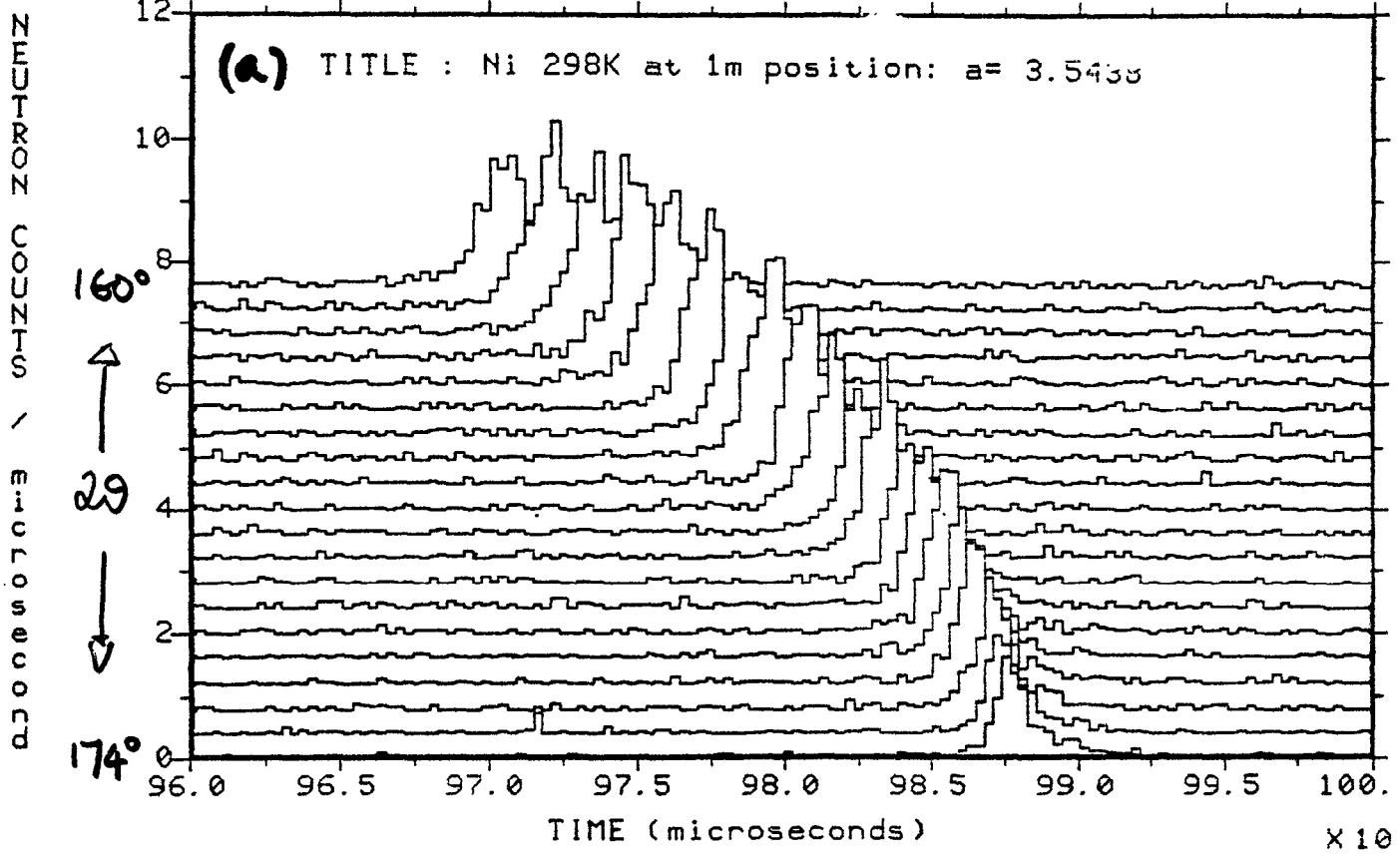
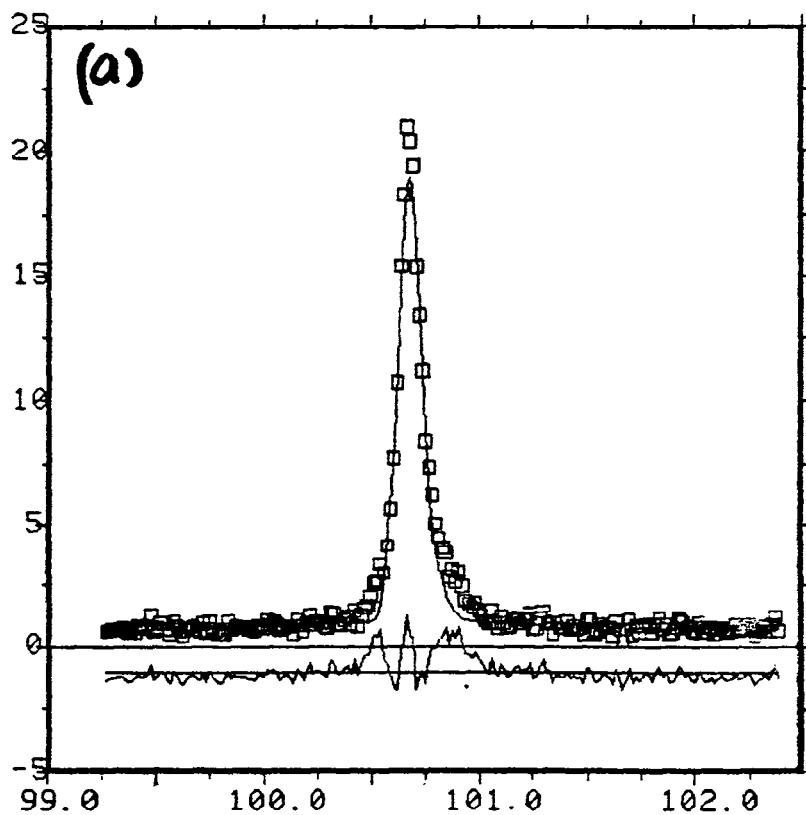


Figure 3: Multispectral plot of the Ni 111 reflection for one detector octant showing (a) the Lorentzian leading edge and (b) the exponential trailing edge. Crosstalk between detector rings is not observed.

TITLE : Ni 298K at 2m position: a= 3.5438 Å

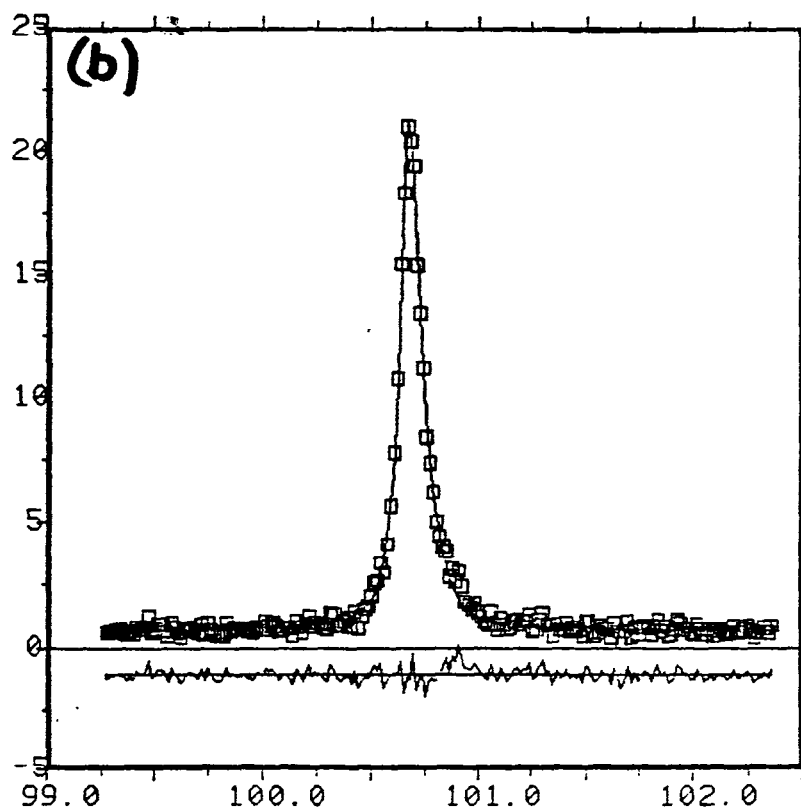


SUBPROGRAM: KROFF.F.EXE

\*\*\* BACKGROUND PARAMETERS \*\*\*  
 intercept = 2.237350 +- 4.12835  
 slope = -0.1318008E-04 +- 0.409412E-04

\*\*\* PEAK PARAMETERS \*\*\*  
 peak area = 2698.432 +- 461.238  
 position = 100643.6 +- 2.50375  
 sigma = 47.20386 +- 1.73795  
 tau = 45.48897 +- 4.02389

R-factor = 1.88 %



SUBPROGRAM: EQL.EXE

\*\*\* BACKGROUND PARAMETERS \*\*\*  
 intercept = -0.3609225 +- 2.10082  
 slope = 0.1052772E-04 +- 0.208333E-04

\*\*\* PEAK PARAMETERS \*\*\*  
 peak area = 3544.456 +- 30.0341  
 position = 100643.1 +- 0.927842  
 FWHM = 76.12152 +- 3.26256  
 tau = 46.84881 +- 1.69370

R-factor = 0.47 %

TOTAL t-to-f (microseconds)

Figure 4: (a) Exponential/Gaussian and (b) Exponential/Lorentzian convolution fits of the 111 Ni diffraction peak. The significantly superior fit of the latter peak shape may be attributed to particle size effects (average = 1710(70) Å).

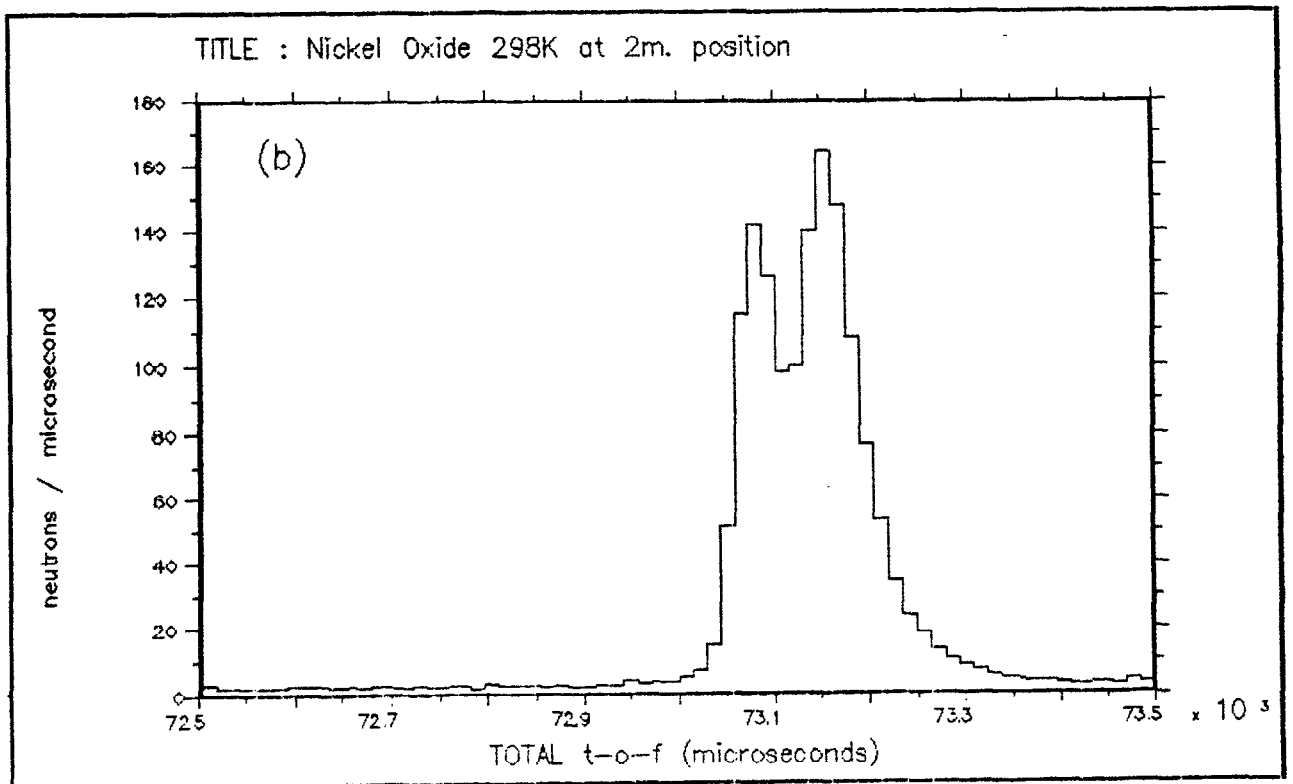
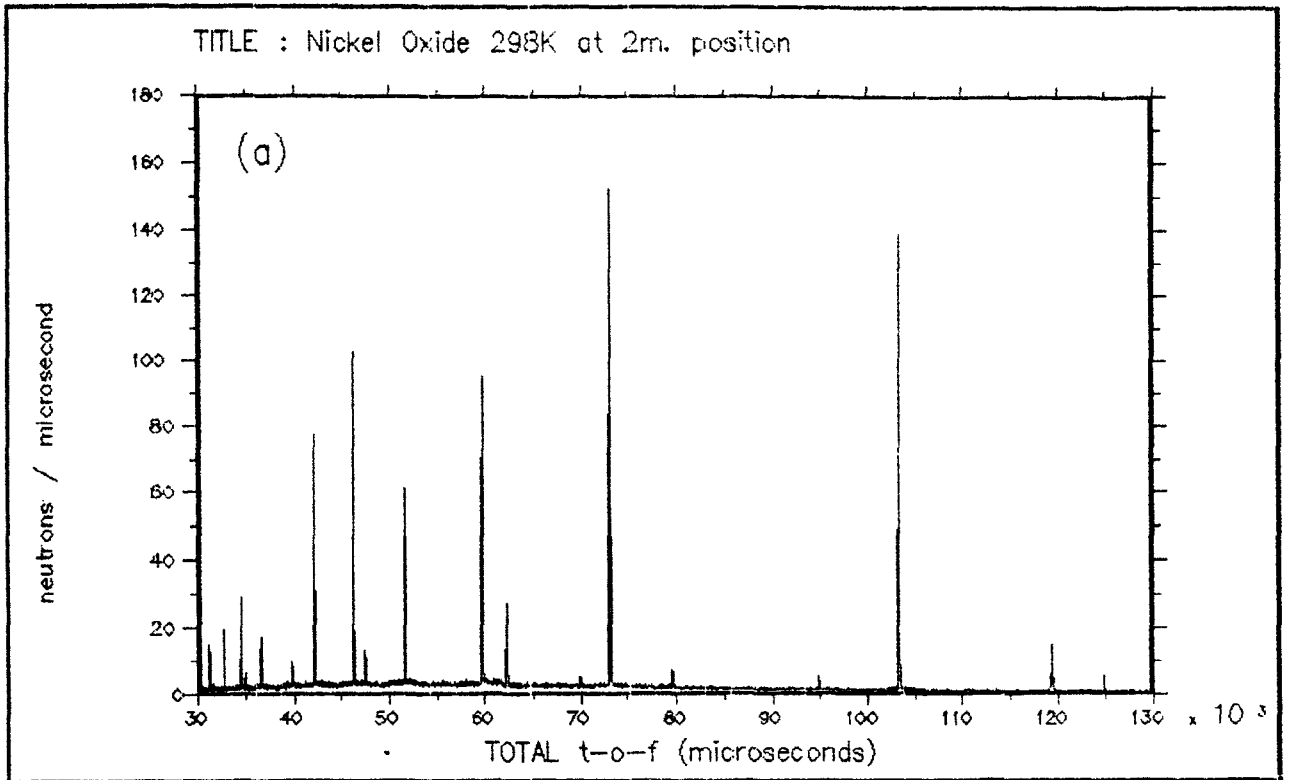


Figure 5: NiO diffraction pattern. (a) The large time range ( $30000 \mu\text{s} < t < 130000 \mu\text{s}$ ) clearly illustrates the good signal-to-noise levels and high resolution of HRPD. (b) The expanded region between  $72500 \mu\text{s}$  and  $73500 \mu\text{s}$  highlights the ultra-high resolution of HRPD. (The time bin-widths are given by the equation  $\Delta t = 0.0002 t$ ).

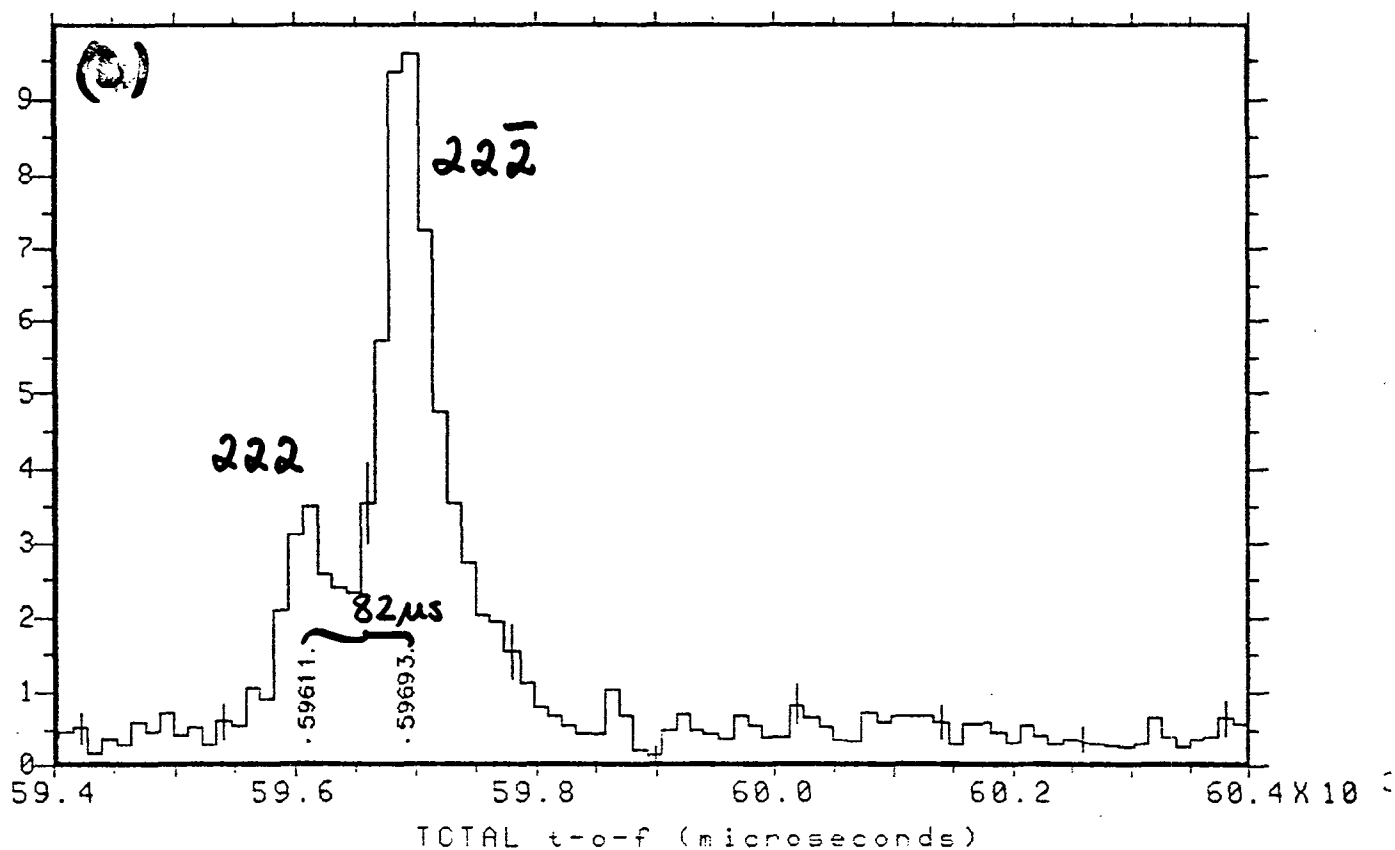
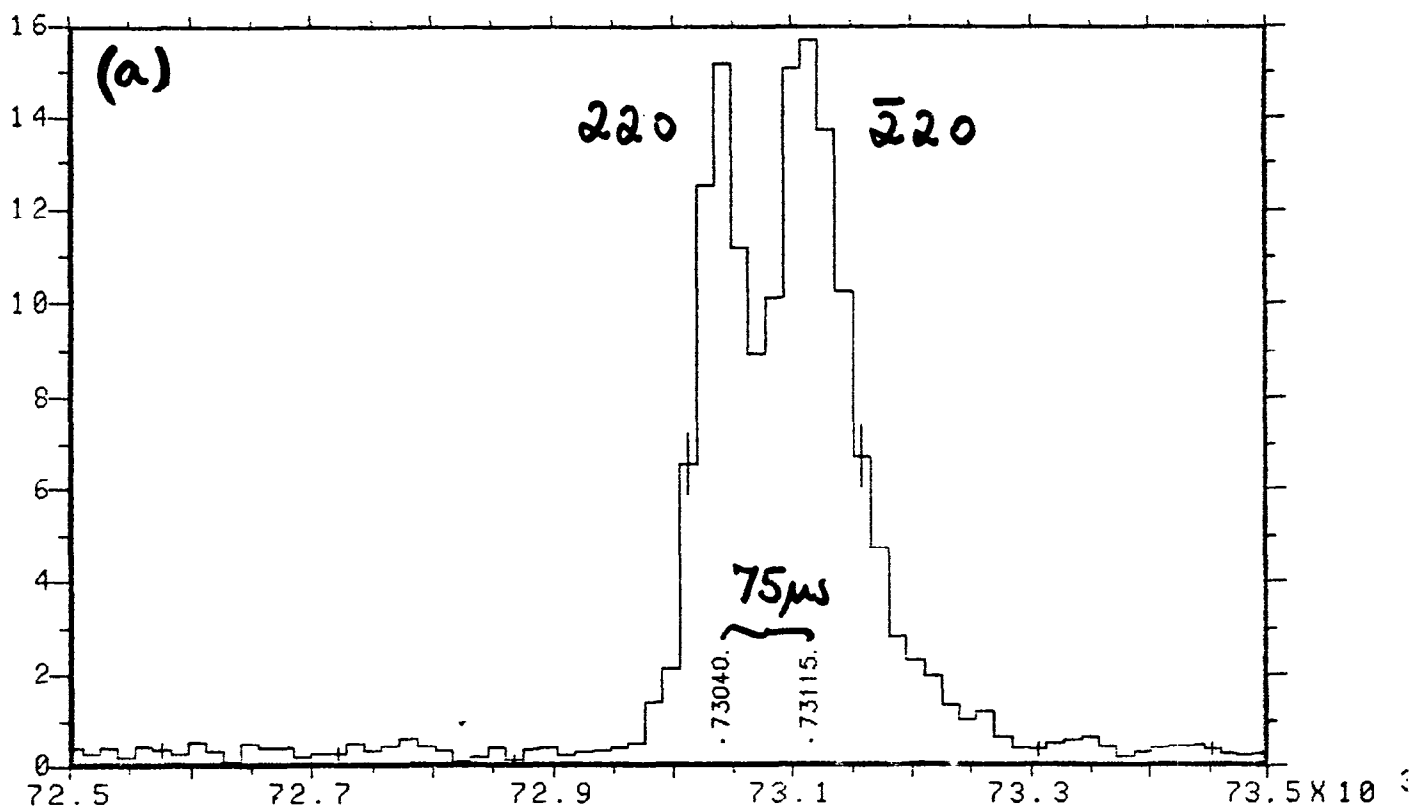


Figure 6: NiO diffraction patterns of (a) 220 splitting and (b) 222 splitting.

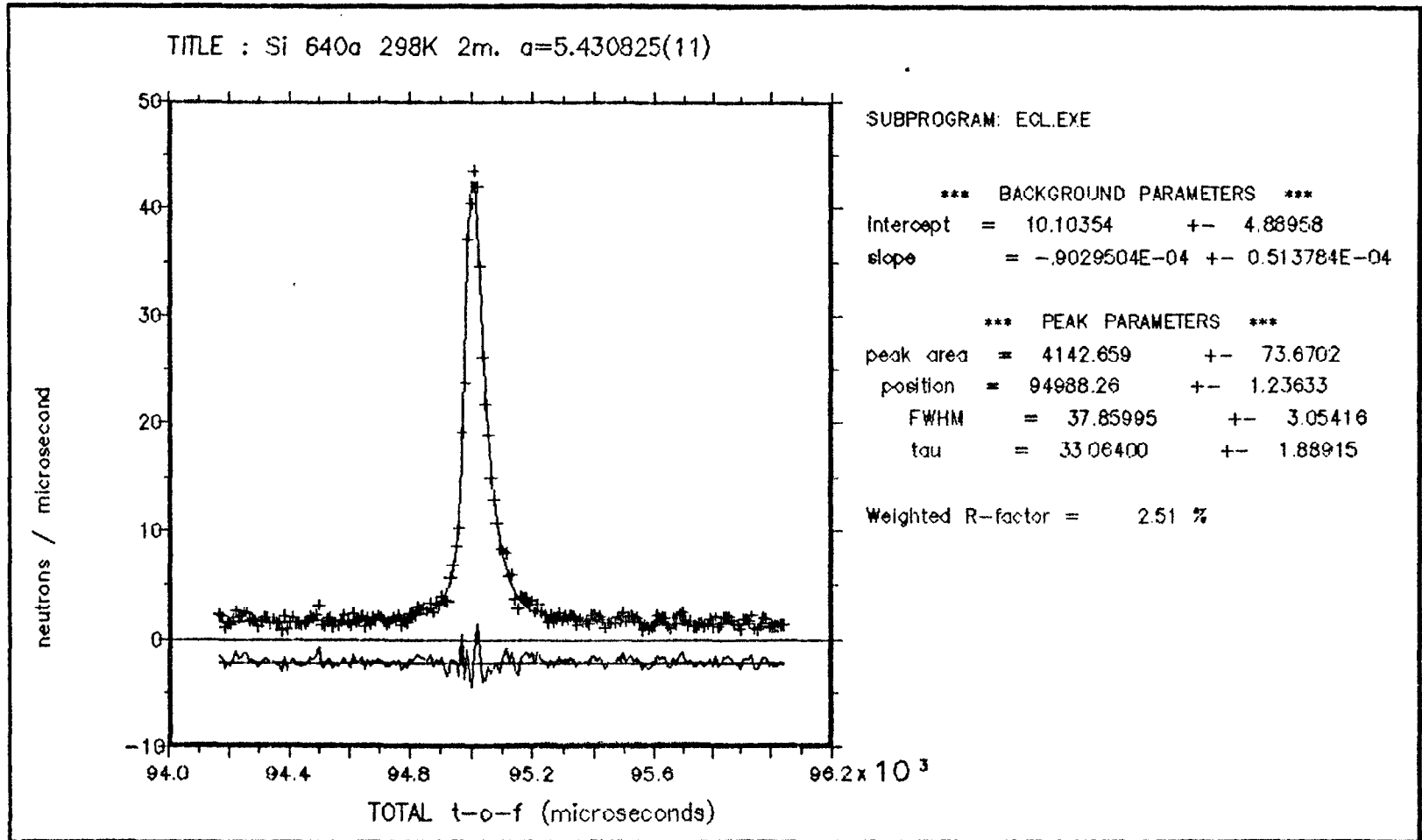


Figure 7: Exponential/Lorentzian fit of the 311 Si peak.

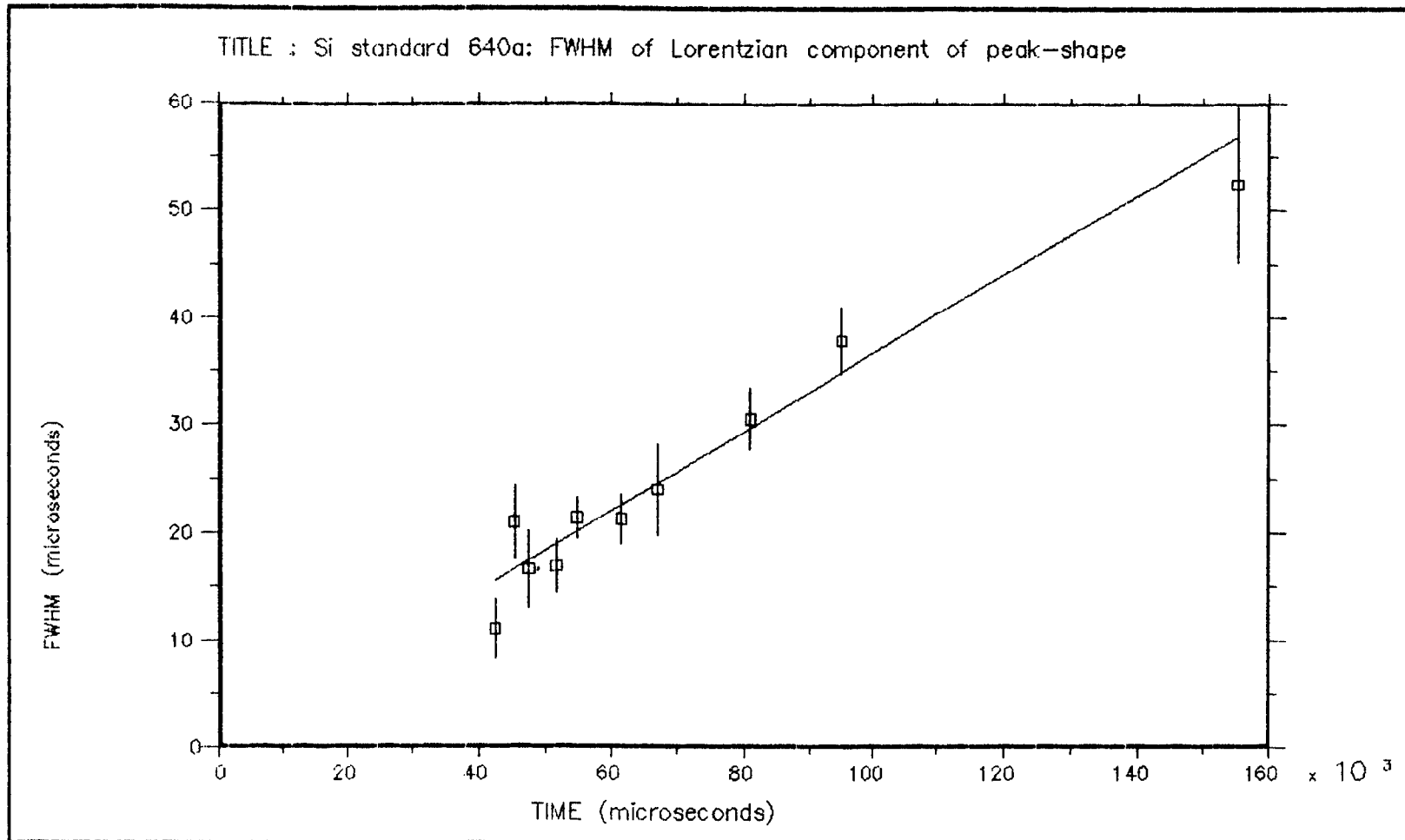


Figure 8: The variation of full width at half maximum of the Lorentzian component of the Exponential/Lorentzian convolution peak shape as a function of time-of-flight.